



Contents lists available at ScienceDirect

Chinese Chemical Letters

journal homepage: www.elsevier.com/locate/cclet



Communication

Hollow Co_9S_8 from metal organic framework supported on rGO as electrode material for highly stable supercapacitors

Peng Wang^{a,b}, Chunyang Li^b, Weigang Wang^b, Jing Wang^b, Yusong Zhu^{b,*}, Yuping Wu^{a,b,*}

^a State Key Laboratory of Materials-Oriented Chemical Engineering, Nanjing Tech University, Nanjing 211816, China

^b School of Energy Science and Engineering & Institute for Advanced Materials, Nanjing Tech University, Nanjing 211816, China

ARTICLE INFO

Article history:

Received 2 January 2018
Received in revised form 24 January 2018
Accepted 25 January 2018
Available online xxx

Keywords:

Cobalt sulfides
Metal organic framework
Reduced graphene oxides
Supercapacitors
Energy storage

ABSTRACT

Metal sulfides as a feasible candidate with high specific capacitance for supercapacitors suffer from sluggish ion/electron transport kinetics and rapid capacitance fading. Herein, we demonstrate a method to fabricate a composite of reduced graphene oxide (rGO) with hollow Co_9S_8 derived from metal organic framework (MOF). Due to the combined highly conductive rGO substrates and hollow shell, the prepared rGO/ Co_9S_8 composite exhibits a high specific capacitance of 575.9 F/g at 2 A/g and 92.0% capacitance retention after 9000 cycles. Its excellent electrochemical performance provides great promise for application, and this versatile method can be extended to prepare other similar nanocomposite.

© 2018 Chinese Chemical Society and Institute of Materia Medica, Chinese Academy of Medical Sciences.
Published by Elsevier B.V. All rights reserved.

Supercapacitors with attractive high power density, rapid charge and discharge and long cycling life have attracted increasing research attentions. As the key components for supercapacitors, electrode materials with high specific capacitance, good rate performance and stable cycling have been widely investigated [1–4]. Porous carbons are one of the widely explored candidates due to their large specific surface area, rich porosity, high electron conductivity and ultrashort charge-discharge time, which is closely related to their energy storage mechanism, i.e., electric double layer instead of Faradaic process [1,2]. However, supercapacitors based on porous carbon materials show limited energy density, and then focus is turned into the investigation of pseudocapacitive materials based on the charge-transfer Faradaic reactions, i.e., redox reactions, such as oxides and sulfides [3,4].

The fast reversible redox reactions, and/or ion intercalation/deintercalation reactions occurring on the shallow surface are supposed to be responsible for high pseudocapacitance [4]. Consequently, nanoscale materials with diverse unique morphology such as hollow structure [4–6], core-shell design [7] and nanosheets [8] holding higher specific surface area compared to their bulk counterparts have been widely explored. On the other side, general pseudocapacitive materials such as metal oxides or sulfides show poor electron conductivity and/or limited cycling

stability, which greatly limit their electrochemical performance and practical applications. The introduction of conductive agents such as carbon nanotubes (CNTs) [9,10] and graphene [4,11,12] enables the remarkable improvement of the electrochemical performance by increasing the electronic conductivity and preventing the collapse of nanostructures during repeated cycling process.

Recently, metal organic framework (MOF) compounds, due to their high specific surface area, controllable abundant porous structure and simple synthesis methods, were investigated for energy storage applications [4,13–15]. For example, a composite of nanoporous Co_3O_4 and carbon with high capacitance was synthesized by a single MOF and ZIF-67 (zeolitic imidazolate framework) was used to prepare electrode materials for supercapacitors with a high capacitance of 504 F/g [16]. The metal sulfides with hollow structure possessing high specific area and ordered porous structure was synthesized via sulfidation of MOF [5,17,18]. These hollow particles show better electrochemical performance compared with their bulk materials. However, they still present poor conductivity. Recent work showed that sandwich-like cobalt sulfide based on reduced graphene oxides (rGO) shows high cycling stability with 99.7% capacitance retention after 4000 cycles [12].

Herein, we reported a simple hydrothermal method to prepare a composite of rGO with hollow Co_9S_8 particles from the reaction of uniform ZIF-67 nanoparticles with thioacetamide and results show that they can be used as superior electrode materials for supercapacitors.

* Corresponding authors at: School of Energy Science and Engineering & Institute for Advanced Materials, Nanjing Tech University, Nanjing 211816, China.

E-mail addresses: zhuys@njtech.edu.cn (Y. Zhu), wuyup@fudan.edu.cn (Y. Wu).

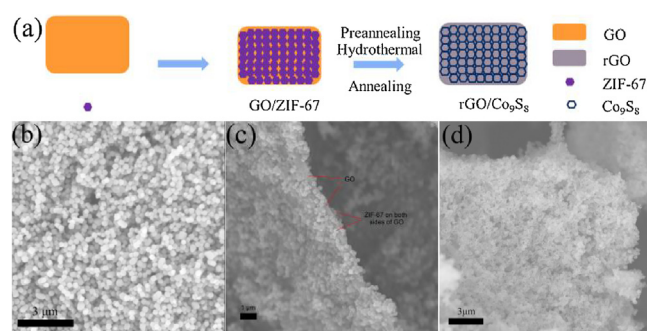


Fig. 1. Schematic illustration of the preparation process of rGO/Co₉S₈ (a) and SEM images of synthesized materials in each process: (b) ZIF-67, (c) GO/ZIF-67, and (d) rGO/Co₉S₈. Scale bar: (a) 3 μm, (b) 1 μm, (c) 3 μm.

The synthetic procedure of this composite, Co₉S₈/rGO, is illustrated in Fig. 1a and details are shown in Supporting information. Firstly, GO was prepared via a chemically modified method [19]. Then, ZIF-67 was prepared by mixing the 2-methylimidazole (2-MI) solution and cobalt nitrate hexahydrate (Co(NO₃)₂·6H₂O), and kept still for 24 h. Monodispersed ZIF-67 with average diameter of 200–300 nm was prepared (Fig. 1b). In the case of the preparation of GO/ZIF-67, beside the addition of GO after adding 2-MI, the process was similar to that of ZIF-67. The obvious composite with uniform ZIF-67 attached to both sides of GO was achieved after the addition of GO [20]. As shown in Fig. 1c, a composite of perfect monodispersed dodecahedron of ZIF-67 supported on GO was prepared. The obtained GO/ZIF-67 composite was dispersed in ethanol solution by ultrasonic treatment, followed by adding thioacetamide (TAA). After hydrothermal reaction at 120 °C for 3 h in a Teflon-lined stainless steel autoclave, the obtained precipitate was annealed at 500 °C in argon atmosphere for 2 h. A composite of rGO with hollow Co₉S₈ particles was successfully prepared (Fig. 1d).

Magnified SEM image of ZIF-67 (Fig. 2a) show clearly that it exists as dodecahedron particles and there is little change in shape from the initial ZIF-67, and that of Co₉S₈ exists as hollow particles (Fig. 2b). Some broken particles also verified the hollow structure of the prepared Co₉S₈. Noteworthy, the average diameter of the obtained Co₉S₈ is enlarged after the sulfidation, which can be explained by the different diffusion speed of metal ion and sulfur ion. During the sulfidation procedure, the sulfur ion dissolved from TAA diffused to the surface of the ZIF-67 and combine the cobalt ion to form a hollow Co₉S₈. Due to the large diameter of sulfur ion it is difficult to move inward. As a result, the smaller cobalt ion moved outward to form cobalt sulfide. Therefore, the inner side of the ZIF-67 particles becomes empty and a hollow Co₉S₈ is achieved (Fig. S1 in Supporting information). As shown in Fig. 2c, powder X-ray diffraction (XRD) patterns for both ZIF-67 and GO/ZIF-67 show typical ZIF topologies, and no peak of GO is observed because of its low intensity. The XRD patterns of Co₉S₈ and rGO/Co₉S₈

(Fig. 2d) show the characteristic peaks of (311), (222), (331), (511) and (440) planes for the cobalt pentlandite (JCPDS No. 86-2273, Co₉S₈) at 2θ values of 29.8°, 31.2°, 39.6°, 47.6° and 52.1°, respectively. Raman spectra (Fig. S4 in Supporting information) show a clear evidence of the presences of graphene in the composites. Raman peaks at 1361.2 cm⁻¹ and 1603.2 cm⁻¹ could be ascribed to disordered carbon-induced D band and graphitic carbon related G band of rGO/Co₉S₈, respectively.

For cobalt sulfide-based electrode in alkaline solution (1 mol/L KOH), the Faradaic reactions are suggested as the following equations [21]:

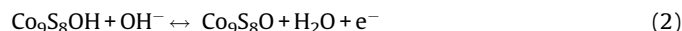


Fig. 3a shows the representative cyclic voltammetric (CV) curves of the rGO/Co₉S₈ at various scan rates in the potential range of 0–0.55 V (vs. saturated calomel electrode, SCE). All of the curves show clear pseudocapacitance features with a similar shape, an evident oxidation peak and a large reduction one, which correspond to the reactions suggested in Eqs. (1) and (2). The curves maintained regular shapes even at a high scan rate of 100 mV/s, indicating the superb high-rate performance of rGO/Co₉S₈. To compare the functions of the added rGO, their CV curves at a scan rate of 10 mV/s are shown in Fig. 3b. The higher area of the closed CV curve of the rGO/Co₉S₈ indicates its higher activities for the redox reactions due to the presence of rGO. When the current density increases from 2 A/g to 10 A/g in the potential window from 0 to 0.45 V (Fig. 3c), there are no obvious potential plateaus, which are similar to those of supercapacitors and different from those of batteries [4,22]. Due to the existence of pseudocapacitance from the redox reactions of Eqs. (1) and (2), their charge and discharge curves are not linearly symmetric [4]. The capacitances of the electrodes were calculated from the following Eq. (3):

$$C_s = \int \frac{Idt}{m\Delta V} \quad (3)$$

where C_s is the specific capacitance (F/g), I is the discharge current (A), dt is the differential of discharge time, m is the mass of the active materials (g) and ΔV (V) is the differential of potential. The rGO/Co₉S₈ electrode shows a specific capacitance of 575.9, 526.0, 493.7, 467.2 and 447.7 F/g at a current density of 2, 4, 6, 8 and 10 A/g, respectively (Fig. 3d). The IR drop of the curves resulting from fast accumulation of charges and reactions during the charge/discharge process is relatively low even at a large current density of 10 A/g. The specific capacitance of the rGO/Co₉S₈ retains 59.9% with the current density ranging from 1 A/g to 20 A/g. This is illustrated from the EIS spectra of Co₉S₈ and the rGO/Co₉S₈, and their corresponding equivalent circuits shown in Fig. 3e. The resistance of the system (R_s), including the ohmic resistance of

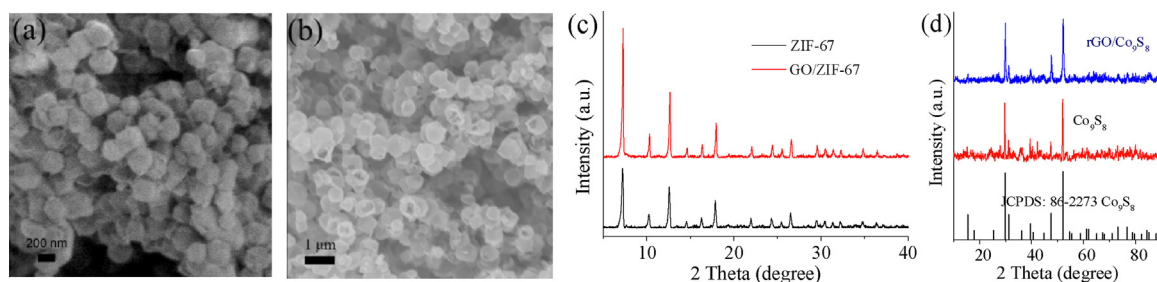


Fig. 2. SEM images of ZIF-67 (a) and Co₉S₈ (b), XRD patterns of ZIF-67 and GO/ZIF-67 (c), and Co₉S₈ and rGO/Co₉S₈ (d).

Download English Version:

<https://daneshyari.com/en/article/7693297>

Download Persian Version:

<https://daneshyari.com/article/7693297>

[Daneshyari.com](https://daneshyari.com)